On the Estimation of the Elastoplastic Work Needed to Initiate Crack Tearing

Luiz Fernando Nazaré Marques
Federal University of South and Southeast of Pará, UNIFESSPA, Avenida dos Ipês s/n, Marabá, 68500-000, Brazil
lfernando@unifesspa.edu.br

Eduardo Enes Cota, Jaime Tupiassú Pinho de Castro, Luiz Fernando Martha, Marco Antonio Meggiolaro
Pontifical Catholic University of Rio de Janeiro, PUC-Rio, Rua Marquês de São Vicente 225, Rio de Janeiro, 22451-900, Brazil
eduardo7cota@hotmail.com, jtcastro@puc-rio.br, lfm@tecgraf.puc-rio.br, meggi@puc-rio.br

ABSTRACT. The elastoplastic frontiers of the plastic zones (*pz*) ahead of the crack fronts is obtained by incremental elastoplastic finite element three-dimensional calculations performed for cracked components with relatively high and low transversal constraints. Such detailed calculations consider all effects associated with the actual cracked component geometry and its loading conditions. From the numerical results, it is shown that, contrary to what is assumed in Fracture Mechanics estimates, the size of the plastic zones can vary significantly for a given Stress Intensity Factor. Since damage ahead of the crack front depends on the *pz* that always form ahead of crack fronts, or is at least much affected by it, this fact cannot be neglected. Indeed, it can have a major importance in practical applications, including in fatigue and in elastoplastic fracture estimates. This work proposes a methodology for evaluating the *pz* volume based on a solid submodeling Finite Element (FE) analysis in which the smallest computation unit is the volume of influence of a plastified Gauss integration point, as opposed to considering an entire plastified FE as the smallest volume unit. Then, assuming that for tough metallic structural alloys their toughness can be obtained from the elastoplastic work needed to initiate crack tearing, the toughness is estimated from the stresses and strains inside the *pz*. In the continuation of this work, such estimates will be compared with toughness values measured at the threshold of crack tearing in highly and lightly constrained specimens following ASTM E1820 testing procedure and an estimation procedure of J-resistance curves, respectively.

KEYWORDS. 3D finite elements; incremental elastoplastic calculations; 3D pz estimates; elastoplastic work; toughness estimates.

INTRODUCTION

The calculation of stress and strain fields around the crack tip in cracked structural components must be accurate because the crack fronts act as 3D stress intensifiers and are the primary cause for crack propagation, stable tearing and unstable fracture in them. Hence, this sort of analysis is important in engineering problems that involve fatigue and fracture analyses. A number of detailed 3D numerical studies to characterize the plastic zones (*pz*) developed around crack fronts and to quantify their effects on the structural integrity of cracked mechanical components are available, see e.g. [1-3]. Such studies have shown that bilinear and trilinear elastoplastic material models provided almost identical results, when considering isotropic and kinematic hardening under monotonic loads [4]. In this work, a constitutive bilinear isotropic hardening model is used to numerically estimate the sizes and shapes of plastic zones in CT and SET specimens, as well as the elastoplastic (EP) stress/strain distributions inside them. A submodeling finite element (FE) technique [5] is adopted in the numerical calculations, using material properties taken from the literature [2]. First, the 3D EP submodeling FE technique was validated through direct comparison with recent numerical and experimental results [2, 3]. Then, the EP frontiers of the *pz* ahead of the crack fronts and the stress/strain distributions inside them were obtained by careful incremental 3D EP submodeling FE analyses performed for some cases of cracked components with relatively high and low transversal constraints around the crack front. These constraints were varied changing the crack size and loading conditions. Geometry parameters are represented by crack length/specimen width (a/W) and specimen width/specimen thickness (W/B). Loading conditions are represented by nominal stress/yield strength (σ_n/S_Y) ratios for constant Stress Intensity Factors (SIF) K_I.

STUDY OF THE 3D PLASTIC ZONE

One of the main objectives of this work is to show that, contrary to what is usually assumed in most Fracture Mechanics estimates, the size of the plastic zones can vary significantly for a given Stress Intensity Factor. Since both the material toughness and its resistance to fatigue crack growth depend on plastic work performed inside the *pz*, this fact can have a major importance in many engineering estimates. Therefore, several numerical FE analyses are performed, varying the parameters of the specimen models, but keeping a constant K_I SIF value. For each simulated geometry, a 3D EP global FE model was generated and meshed using more refined elements around the crack and increasing their size in regions away from the crack. Middle tension (MT), compact tension (CT) and Single Edge Tension (SET) specimens were used in this study. From the solution of the global model, the EP frontiers of the *pz* in terms of the equivalent Mises strain was mapped in order to ensure that the total volume of the *pz* is entirely within the submodel with meshes of uniform element size for the final solution. The properties of the materials used in all simulations are presented in Tab. 1.

Material	E [GPa]	ν [1]	S_Y [MPa]	H [MPa]	h[1]	H' [MPa]	H/E [1]
2024-T3	73.1	0.33	345	-	-	984	-
2024-T351	73.5	0.33	425	685	0.073	220.5	0.003

Table 1: Materials and properties [2, 3].

For all the traditional specimens selected for this study, there are well-known expressions for K_I available in the literature: $K_I = P/(B\sqrt{W})f(a/W)_{Specimen}$, where $f(a/W)_{Specimen}$ is a geometry function that depends on the crack size (a) to specimen width (W) ratio. The equations 1-3 present these functions for the cracked components CT [6], MT [7] and SET [7].

$$f\left(\frac{a}{W}\right)_{CT} = \frac{\left(2+\frac{a}{W}\right)}{\left(1-\frac{a}{W}\right)^{3/2}}\left[0.886+4.64\left(\frac{a}{W}\right)-13.32\left(\frac{a}{W}\right)^2+14.72\left(\frac{a}{W}\right)^3-5.6\left(\frac{a}{W}\right)^4\right] \quad (1)$$

$$f\left(\frac{a}{W}\right)_{MT} = \sqrt{\left(\frac{\pi a}{4W}\right)\sec\left(\frac{\pi a}{2W}\right)}\left[1-0.025\left(\frac{a}{W}\right)^2+0.06\left(\frac{a}{W}\right)^4\right] \quad (2)$$

$$f\left(\frac{a}{W}\right)_{SET} = \frac{\sqrt{2\tan\left(\frac{\pi a}{2W}\right)}}{\cos\left(\frac{\pi a}{2W}\right)}\left[0.752 + 2.02\left(\frac{a}{W}\right) + 0.37\left(1 - \sin\frac{\pi a}{2W}\right)^3\right] \quad (3)$$

Numerical validation

To validate the FE numerical analysis, a comparison is made to two recent three-dimensional results taken from the literature [2, 3] for MT and for CT specimens. Geometry and loading of these specimens are summarized in Tab. 2. References [2, 3] used 3D SOLID185 elements with 8 nodes each, 8 Gaussian integration points per element and 3 degrees of freedom per node. In this work, the ANSYS software was used. For comparison, the same type of element of those references was adopted in the submodel that contains the *pz*. In the global model, since a less refined mesh is required, it uses larger 3D SOLID186 elements with 20 nodes each, 8 Gaussian integration points per element. A mesh convergence study (not shown here) was performed based on evaluations of the total volume (V_t) of the *pz* developed around the crack front for different mesh sizes. For a local analysis of stress and strain fields, it is recommended to apply a denser mesh at least around the crack front, as already suggested in many studies [1, 8, 9].

Specimen	a/W [1]	a [mm]	W [mm]	W/B [1]	P [kN]	K_I [MPa√m]	σ_n/S_Y [%]
MT	0.25	20.00	80.00	16.00	92.14	30.00	33.00
				40.00	36.86		
				16.00	61.43	20.00	22.00
				40.00	24.57		
CT	0.74	54.00	72.50	12.08	1.49	25.00	80.50
				24.17	0.75		
				7.25	1.77	17.82	57.38

Table 2: Cases published in the literature [2, 3].

Figure 1 shows the shapes and volumes of only 1/4 of the pz on a MT specimen for K_I = 30MPa√m for two thickness conditions. Reference [2] estimates the size of the *pz* based on the FEs that have Mises stress higher than S_Y in one of its integration points. The same criterion was adopted here and a similar value for V_t (19.96mm³) for the specimen MT with thickness B = 5mm was obtained. Figure 2 shows the numerical vertical displacements around the crack front on a CT specimen with 10mm thickness for K_I = 17.82MPa√m at three different vertical levels, and compares these results with those obtained from reference [3].

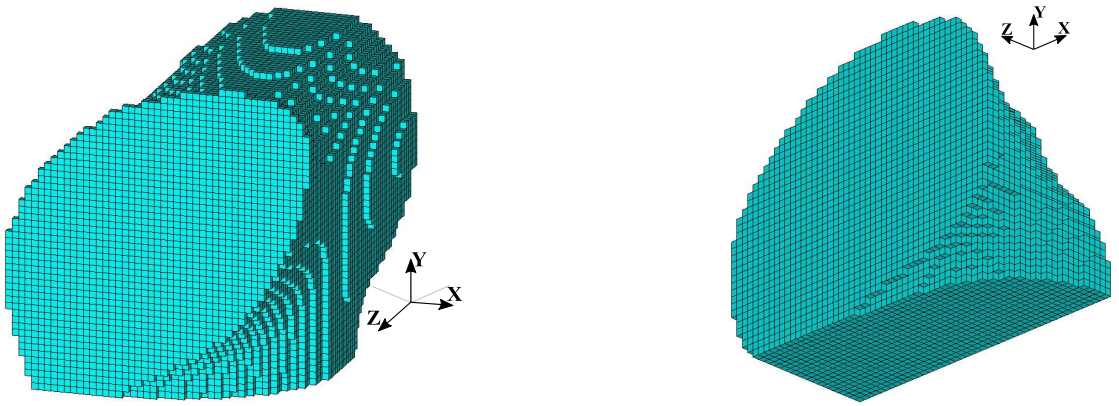

a) b)

Figure 1: 1/4 shape and volume of the *pz* developed around the crack front on MT component for K_I = 30MPa√m: a) B = 5mm; e b) B = 2mm.

In spite of the good agreements with those references results, the criterion for selection of the smallest unit considered in the *pz* can be improved. The smallest unit of volume considered in the *pz* was the volume of the element (V_e) adopted in the modeling. In this case, even when only one Gauss integration point was plastified ($\varepsilon_{eq} \geq \varepsilon_Y$) at the elastoplastic frontiers of the *pz*, the entire element was counted in the *pz* volume. This methodology adopted to calculate the volume of the *pz* can lead to different values when using linear elements and coarse meshes. This verification was carried out through numerical experiments performed using a simply supported beam uniformly loaded, which has an analytical solution [10]. Quadratic elements were in these FE simulations, and only the fractions of the volumes corresponding to their plastified Gauss integration points were counted as part of the *pz* around the crack tips. Thus, the smallest unit of volume treated in the *pz* models became $V_e/8$.

All numerical simulations were performed considering only 1/4 of the modeled specimens due to their symmetries, and using the following geometric and material parameters: L = 300mm, L/B = 10, B/H = 1, E = 210GPa, S_Y = 300MPa, ν = 0.3, $P_0 = 4BS_Y$, and $\rho = (P/P_0)(L/H)^2$, where P is the uniformly applied load, ρ defines the percentage of the cross section plastification and $2L$, $2B$ and $2H$ are the beam length, thickness and height, respectively. Figure 3 shows the variations of the relative errors between the analytical (V_a) and numerical (V_n) plastic volumes as a function of the number of elements along B. Fig. 4 shows the analytical and numerical elastoplastic frontiers of the plastic volumes considering a partial (ρ = 0.8) and a fully plastic cross section (ρ = 1.05). Comparisons between numerical analysis and analytical solutions indicate good correlations when the smallest unit of volume treated in the pz is $V_e/8$. The relative error between V_a and V_n is reduced from 35% to 6% using the improved criterion, as can be seen in Fig. 3.

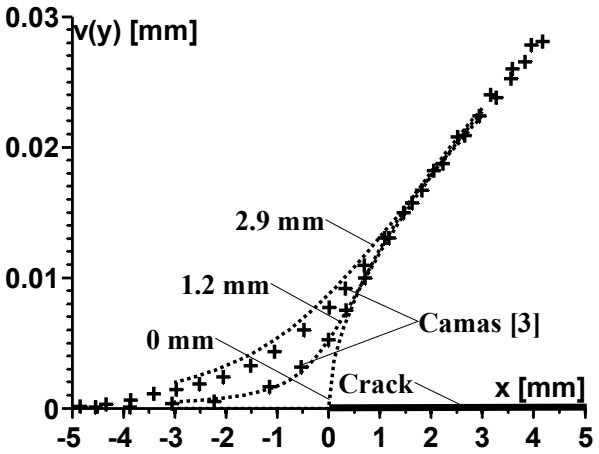

Figure 2: Numerical vertical displacement on CT component for K_I = 17.82MPa√m at the crack plane, 1.20mm and 2.90mm from the crack plane.

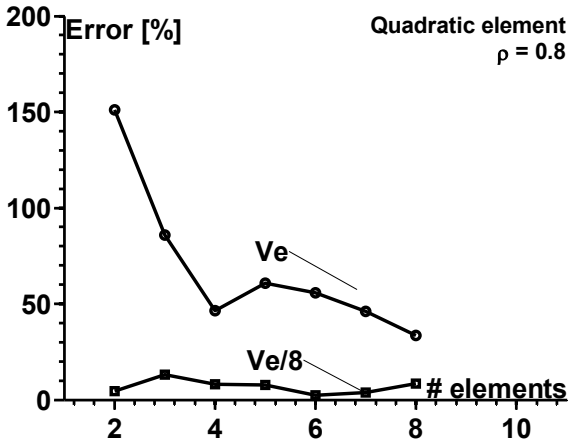

Figure 3: Errors between the analytical (V_a) and numerical (V_n) plastic volumes counting the entire volume of the element (V_e) and its fraction ($V_e/8$) in the *pz* volume for a partial cross section (ρ = 0.8).

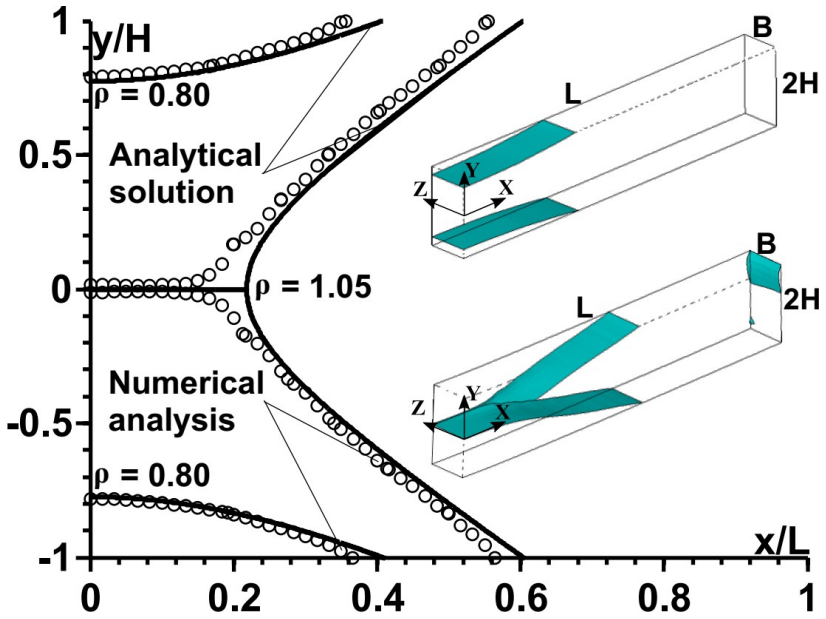

Figure 4: Elastoplastic frontiers for a partial ($\rho = 0.8$) and a fully plastic cross section ($\rho = 1.05$).

HIGHLY AND LIGHTLY CONSTRAINED SPECIMENS

To verify the proposed methodology of evaluating $p\tilde{z}$ based on the volume of influence of each plastified Gauss point, such estimates should be compared with toughness values measured at the threshold of crack tearing in highly (CT) and lightly (SET) constrained specimens following ASTM E1820 testing procedure and an estimation procedure of J-resistance curves, respectively. For CT and SET specimens with $K_I = 30\text{MPa}\sqrt{\text{m}}$, Fig. 5 shows the variation along B of the dimensionless ratio between the volume distribution of $p\tilde{z}$ in slices of constant thickness and the volume of the element (V_s/V_e), for 6 cases represented by a SET ($a/W = 0.2$; $\sigma_n/S_Y = 0.3$) and a CT ($a/W = 0.4$; $\sigma_n/S_Y = 0.8$), varying W/B (8, 12 and16). Besides the cases presented in Fig. 5, there are 21 more cases as can be seen in Fig. 6, which shows that the volume of the $p\tilde{z}$ ahead of the crack front represented by the dimensionless ratio between the total volume of $p\tilde{z}$ and the volume of the element (V_t/V_e) can vary significantly for a given K_I. A remarkable difference in this ratio can be seen through a comparison between two cases: a SET specimen with geometry and loading ratios $W/B = 8$, $a/W = 0.4$, and $\sigma_n/S_Y = 0.3$ and a CT specimen with $W/B = 8$, $a/W = 0.4$, and $\sigma_n/S_Y = 0.8$. A surprisingly large factor of 9.6 was observed between them. Hence, based on damage arguments ahead of the crack front, it is possible to argue that J_{IC} measured toughness values may also dramatically change in those specimens.

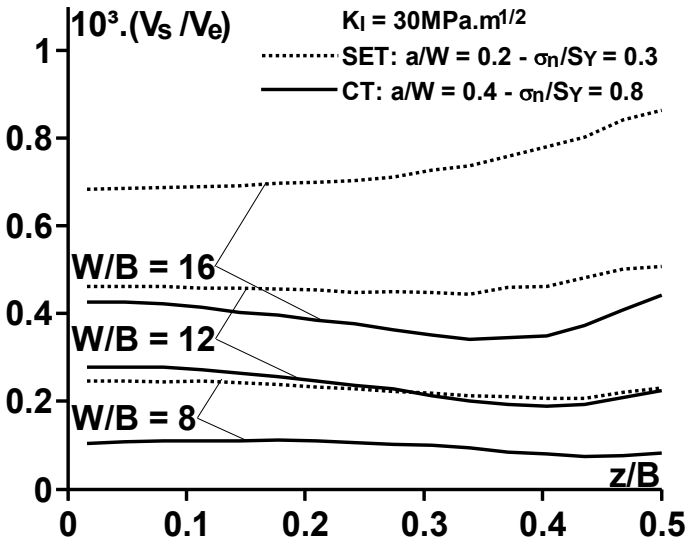

Figure 5: pz volumes along the thickness.

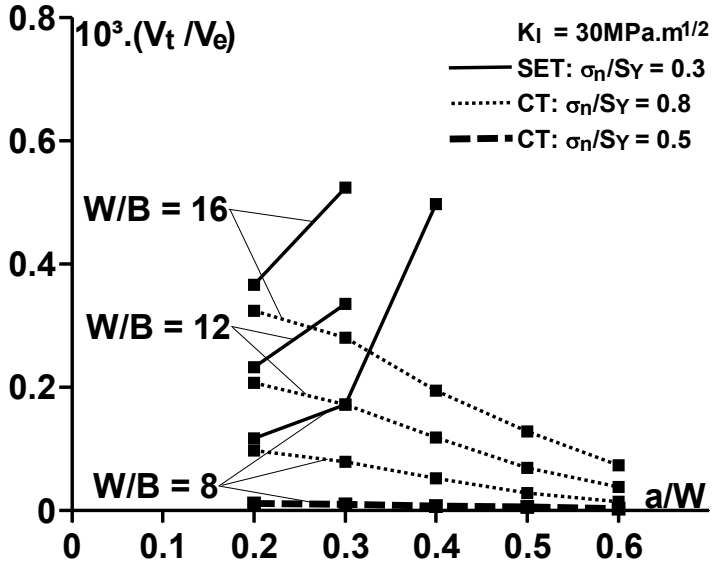

Figure 6: Total pz volumes ahead of the crack front for several simulated cases.

CONCLUSIONS

This work presents 3D pz estimates using a 3D EP submodeling FE technique. The results obtained using this technique were validated through direct comparison with numerical results found in the literature that also contain experimental results for pz sizes and displacements measured on the surface of the specimens using Digital Image Correlation (DIC) techniques. In addition, the methodology for the calculation of pz volumes considering $V_e/8$ as the smallest unit of volume treated in the pz simulation was verified through numerical experiments validated by analytical solutions. Finally, it was observed from the results that for a given K_I the pz volumes are considerably different for several cases, which also implies different values of elastoplastic work in these volumes and, consequently, probably in their fracture toughnesses as well. In conclusion, estimation of fracture toughness from measured pz, both numerically and experimentally, is the major objective of this ongoing work, and it will be further discussed elsewhere.

REFERENCES

[1] D.Camas, J.Garcia-Manrique and A.Gonzalez-Herrera. Numerical study of the thickness transition in bi-dimensional specimen cracks. International Journal of Fatigue, 33 (2011) 921-928.
[2] Michael Besel , Eric Breitbarth. Advanced analysis of crack tip plastic zone under cyclic loading. International Journal of Fatigue, 93 (2016) 92–108.
[3] Camas D et al. Numerical and experimental study of the plastic zone in cracked specimens. Engineering Fracture Mechanics, 185 (2017) 20-32.
[4] Zapatero J, Gonzalez-Herrera A. Advances in the numerical modelling of fatigue crack closure using finite elements. In: Lignelli AF, editor. Fatigue crack growth mech behav predict. New York: Nova Science Publishers; 2009. p. 83–124.
[5] ANSYS 13.1 help//Mechanical APDL (formerly ANSYS)//Advanced analysis techniques guide//9. Sub modeling.
[6] ASTM E1820–17, "Standard Test Method for Measurement of Fracture Thoughness", American Society for Testing and Materials, 2017.
[7] T. L. Anderson, Fracture Mechanics: Fundamentas and Aplications, third ed., Taylor & Francis, (2005).
[8] Anderson, T. L. and Dodds, R. H., Jr., "Specimen Size Requirements for Fracture Toughness Testing in the Transition Region," Journal of Testing and Evaluation, 19 (1991) 123-134.
[9] Graba M., Gatkiewick J., Influence of crack Tip Model on Results of the Finite Element Method, Journal of Theoretical and Applied Mechanics, 45 (2007) 225-237.
[10] Prager and P. G. Hodge, Jr., Theory of Perfectly Plastic Solids, John Wiley & Sons, New York, (1951).